Investigating Balancing Control of a Standing Bipedal Robot With Point Foot Contact

B. Ding*, A. Plummer, P. Iravani

**Centre for Power Transmission and Motion Control, Dept. of Mech. Engineering, University of Bath, Bath, BA2 7AY UK (e-mail: B.Ding@bath.ac.uk)*

Abstract: Comparing with wheeled or tracked moving machines, legged robots have potential advantages, especially when considering moving on discontinuous or rough terrain. For many bipedal robots, balance in the standing position is easy to maintain by having sufficient contact area with the ground. For some bipedal robots, the Zero Moment Point (ZMP) control method has been successfully implemented in which the center of mass is aligned above the support area. However, the balancing issue while standing becomes challenging when the contact area is very small. This paper presents a controller which is developed to balance a bipedal robot with coupled legs which has point foot contact. It is necessary to investigate the non-linear characteristics of the system. A pole-placement control method is used, and noise issues with sensing higher motion derivatives are investigated The simulation-based evaluation indicates limitations that need to be addressed before experimental implementation.

Keywords: center of mass (CoM), balance, bipedal robot, pole placement

1. INTRODUCTION

Considering moving on rough terrain, such as soft and uneven surfaces, legged robots have potential advantages comparing with wheeled or tracked vehicles (Hardarson, 1970). The isolated foot support area avoids the requirement forcontinuous ground.In the last few decades, bipdal robots have attracted researchers` attention. Several successful two-leg walking robots have been presented to show the motion mechanism principles, such as Asimo (Sakagami, 2002), ATLAS and PETMAN (Raibert, 2010). Considering the standing position, most of these platforms solve the balancing problem by having sufficient foot contact area with the ground. The Zero Moment Point control method has been successfully implemented to maintain balance by controlling the centre of mass above the support area while the robot is standing or slowly walking (Erbatur, 2002). An intermittent control strategy might be a solution to solve the body sway issue with a smaller foot contact (Bottaro, 2005). However, the problem is still very challenging when the support area is limited to point contact.

The Bath Bipedal Hopper (BBH) is a small size hydraulic actuated bipedal hopping robot, which is developed to design and test advanced controllers. The foot support area of the BBH is very small, and can be approximated by a point. One mode of operation is balancing while standing rather than hopping, and control for this mode is considered in this paper. A double inverted pendulum model is used to represent the BBH. A pole-placement controller is developed and tested in simulation. Evaluation indicates the feasibility of this method and makes suggestions for further research.

2. HARDWARE OF THE BATH BIPEDAL HOPPER

As Fig. 1 shows, the basic design concept of the BBH comes from kangaroos, which are the largest animal using a bipedal hopping mechanism on the planet. The BBH has an upper body and two lower legs. The upper body consists of a main controller, which is an industrial PC (PC104 format), a manifold integrated with proportional valves and supporting framework. A hydraulic cylinder actuates the fore-aft hip rotation of both legs, i.e. this motion of the legs is coupled together. The two lower legs are hydraulic actuators with position sensors in parallel. There is an inertia measurement unit (IMU) attached with the upper body to measure the body rotation angel. An encoder is used to measure the angle at the hip point. Each foot consists of an aluminium alloy hemisphere covered in hard rubber. The BBH was designed to achieve locomotion using kangaroo-like hopping.. Fig. 2 shows a simplified 3D model of BBH.

Include a table of key dimensions / parameter valves (cylinders, valves, working pressure masses …)

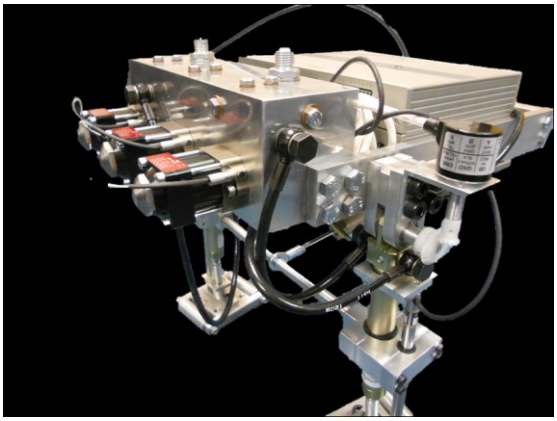

Fig. 1. Hardware of the Bath Bipedal Hopper

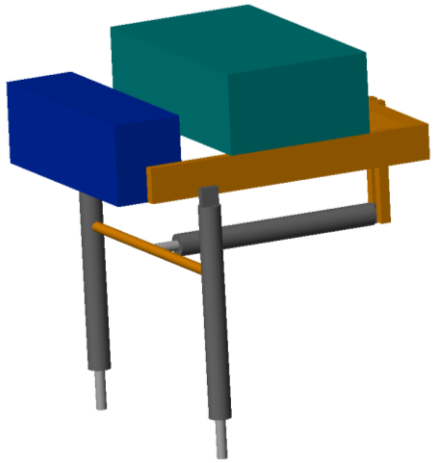

Fig. 2. Simplified 3D model of the BBH

3. MODELLING

3.1 Double inverted pendulum model

The inverted pendulum model has been successfully used to help design one-leg hopping robots (Kajita, 1989). A double inverted pendulum model is appropriate to analyse the motion of the BBH. As shown in Fig. 3, the model consists of two rigid bodies, an upper body and a lower body (representing the leg-pair), connected with revolute joint 1 (hip joint). The bottom of the lower body, i.e. the foot,is connected to the ground using revolute joint 2 in the model. Using small angle approximations, we are trying to maintain the combined Centre of Mass (CoM) of the overall model vertically above revolute joint 2 by applying an active torque at revolute joint 1.

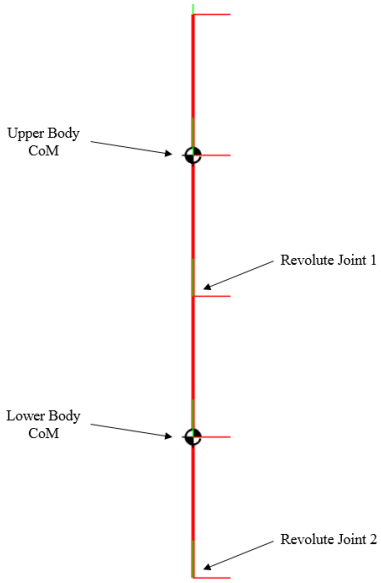

Fig. 3. Double inverted pendulum model

3.2 Dynamic analysis

The force analysis of the upper body is shown in Fig. 4.

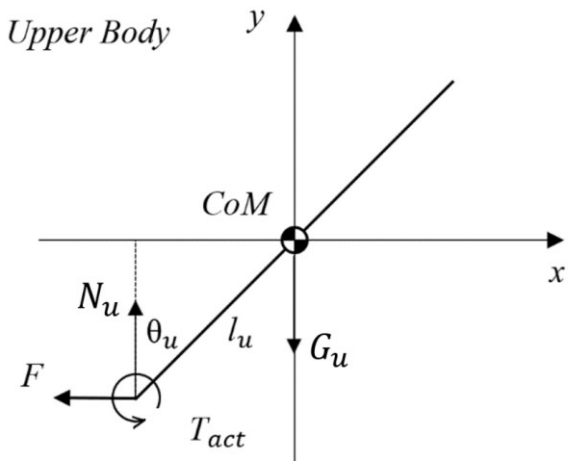

Fig. 4. Upper body force analysis *(put this figure at bottom of page)*

Consider the force on upper body and taking moments about the revolute joint 1 gives (1), (2) and (3):

$$-F = M_u(l_u\ddot{\theta}_u + l_l\ddot{\theta}_l) \tag{1}$$

$$T_{act} - M_u g l_u \theta_u = J_u\ddot{\theta}_u \tag{2}$$

$$J_u = \frac{1}{3}M_u(2l_u)^2 \tag{3}$$

where, M_u is the mass of upper body, l_u is length from the upper body`s CoM to revolute joint 1, l_l is the length of lower body, J_u is the moment of inertia of upper body. Combine (1), (2) and (3) gives:

$$\frac{\theta_u}{T_{act}} = \frac{3}{4M_u l_u^2 s^2 + 3M_u g l_u} \tag{4}$$

Fig. 5 presents the force analysis of the lower body; taking moment about revolute joint 2 gives (5) and (6).

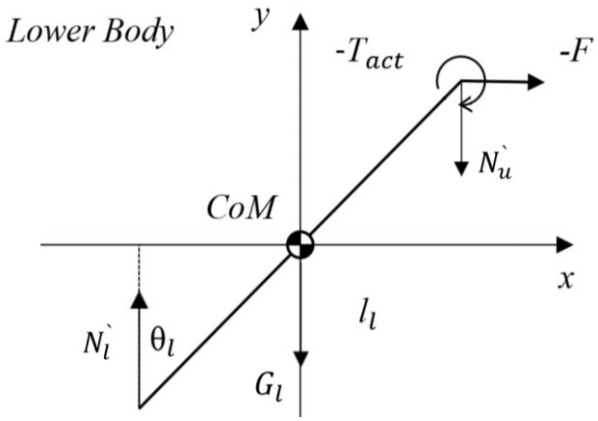

Fig. 5. Lower body force analysis *(put Figs 5 and 6 at bottom of page)*

$$-Fl_l - M_u g l_l \theta_l - \frac{1}{2} M_l g l_l \theta_l = J_l \ddot{\theta}_l \quad (5)$$

$$J_l = \frac{1}{3} M_l l_l^2 \quad (6)$$

M_l is the mass and J_l is the moment of inertia of the lower body. Combining (1), (5) and (6) gives:

$$\frac{\theta_u}{\theta_l} = \frac{(\frac{1}{3} M_l l_l - M_u l_l)s^2 + M_u g + \frac{1}{2} M_l g}{M_u l_u s^2} \quad (7)$$

Considering the overall model, the combined CoM position is shown in Fig. 6.

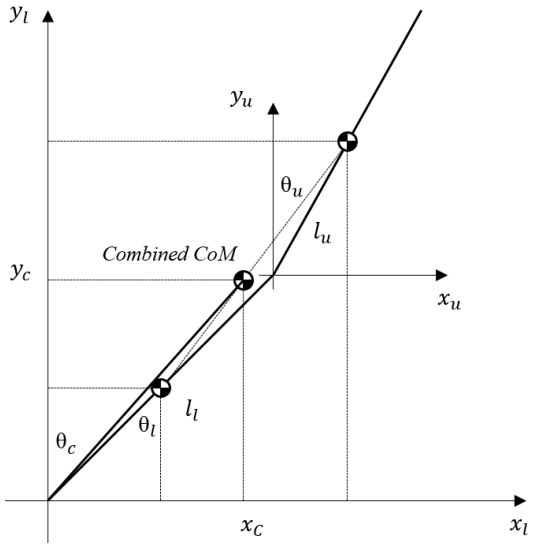

Fig. 6. Position of combined CoM

According to the geometry relations, the position of the combined CoM can be expressed as (8) and (9):

$$x_c = (\frac{1}{2} l_l \theta_l + l_u \theta_u) \frac{M_l}{M_l + M_u} + \frac{1}{2} l_l \theta_l \quad (8)$$

$$y_c = (\frac{1}{2} l_l + l_u) \frac{M_l}{M_l + M_u} + \frac{1}{2} l_l \quad (9)$$

Considering small angle approximation:

$$\tan\theta_c = \frac{x_c}{y_c} = \frac{l_l \theta_l (2M_l + M_u) + 2 l_u \theta_u M_l}{l_l (2M_l + M_u) + 2 l_u M_l} \approx \theta_c \quad (10)$$

If,

$$p = \frac{2 l_u M_u}{l_l (2M_u + M_l)} \quad (11)$$

Then,

$$\theta_c = k_1 \theta_l + k_2 \theta_u \quad (12)$$

Where,

$$k_1 = \frac{1}{p+1} \quad (13)$$

$$k_2 = \frac{p}{p+1} \quad (14)$$

Combining (4), (7) and (12) gives the plant model:

$$\frac{\theta_c}{T_{act}} = \frac{3k_2 k_{l1} s^2 + 3k_1 k_{u3} + 3k_2 k_{l2}}{4k_{u1} k_{l1} s^4 + (k_{l1} k_{u2} + 4k_{u1} k_{l2}) s^2 + k_{u2} k_{l2}} \quad (15)$$

where,

$$k_{u1} = 4M_u l_u^2$$

$$k_{u2} = 3M_u g l_u$$

$$k_{u3} = M_u l_u$$

$$k_{l1} = \frac{1}{3} M_l l_l - M_u l_l$$

$$k_{l2} = M_u g + \frac{1}{2} M_l g$$

4. CONTROLLER DESIGN

According to the plant model, the pole-placement method can be used to develop the controller. The closed-loop block diagram is shown in Fig. 7.

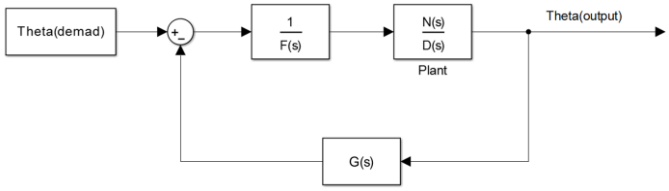

Fig. 7. Block diagram of pole-placement controller

The controller is implemented using two digital filters, $1/F(s)$ and $G(s)$, where $1/F(s)$ is a forward path compensator and $G(s)$ plays the same role as the state feedback gains in a state-feedback controller. The closed-loop transfer function of the above block diagram is:

$$\frac{\theta_c}{\theta_d} = \frac{N(s)}{D(s)F(s) + N(s)G(s)} \quad (16)$$

If,

$$A(s) = D(s)F(s) + N(s)G(s) \quad (17)$$

Then,

$$\frac{\theta_c}{\theta_d} = \frac{N(s)}{A(s)} \quad (18)$$

The roots of polynomial $A(s)$ indicate the stability and the time domain response of the whole system. By specifying different polynomials of $G(s)$ and $F(s)$, the roots of $A(s)$ can be arranged at any desired positions. According to the plant model:

$$N(s) = n_2 s^2 + n_0 \tag{19}$$

$$D(s) = d_4 s^4 + d_2 s^2 + d_0 \tag{20}$$

It is necessary to have the same number of equations and unknowns, which determines the degrees of polynomials $G(s)$ and $F(s)$ (Plummer, A. R. 1991). *Define n and m.* Using,

$$\deg F(s) = n - 1 = 1 \tag{21}$$

$$\deg G(s) = m - 1 = 3 \tag{22}$$

$$\deg A(s) = n + m - 1 = 5 \tag{23}$$

Therefore,

$$F(s) = f_1 s + f_0 \tag{24}$$

$$G(s) = g_3 s^3 + g_2 s^2 + g_1 s + g_0 \tag{25}$$

$$A(s) = a_5 s^5 + a_4 s^4 + a_3 s^3 + a_2 s^2 + a_1 s + a_0 \tag{26}$$

The variables in $G(s)$ and $F(s)$ can be calculated from solving (17) with polynomials as given in (19), (20), (24), (25) and (26), i.e. solving the following matrix equation:

$$\begin{bmatrix} a_5 \\ a_4 \\ a_3 \\ a_2 \\ a_1 \\ a_0 \end{bmatrix} = \begin{bmatrix} d_4 & 0 & n_2 & 0 & 0 & 0 \\ 0 & d_4 & 0 & n_2 & 0 & 0 \\ d_2 & 0 & n_0 & 0 & n_2 & 0 \\ 0 & d_2 & 0 & n_0 & 0 & n_2 \\ d_0 & 0 & 0 & 0 & n_0 & 0 \\ 0 & d_0 & 0 & 0 & 0 & n_0 \end{bmatrix} \times \begin{bmatrix} f_1 \\ f_0 \\ g_3 \\ g_2 \\ g_1 \\ g_0 \end{bmatrix} \tag{27}$$

$A(s)$ will be chosen as the denominator of a fifth order Butterworth filter. A Butterworth filter has a flat frequency response in the passband (). Therefore, determining the vector of $G(s)$ and $F(s)$ coefficients gives a controller achieveing these desired closed-loop poles.

A simple simulation test can be done by using the physical configuration parameters of the BBH, as Table 1 shows.

Table 1. Physical parameters

Parameters	Symbol	Value	Unit
Mass of the upper body	M_u	7.5	kg
Mass of the lower leg	M_l	0.75	kg
Length of the upper body	l_u	44.4	mm
Length of the lower leg	l_l	95	mm
Gravitational acceleration	g	9.81	m/s^2

Fig. 8 shows the step response with these parameters. With a higher cut-off frequency, the system presents a faster step response (as expected) and acceptable overshoot.

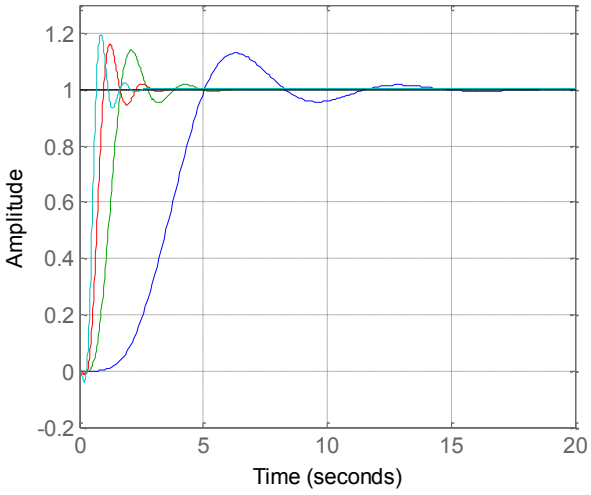

Fig. 8. Step response with closed-loop poles for cut-off frequencies of7 rad/s, 5 rad/s, 3 rad/s and 1 rad/s.

5. EVALUATION OF THE CONTROLLER

5.1 Minimize the jerk gain

There are four unknowns in $G(s)$, which are the feedback gains related to the output angle, angular velocity, angular acceleration and the derivative of angular acceleration, also named the jerk. It is necessary to minimize the jerk gain, or even make it as zero, because of the noise caused by derivative calculations. By setting the jerk gain as zero, $G(s)$ is going to be a second order polynomial and $F(s)$ can be a constant value. Such as:

$$F(s) = f_0 \tag{28}$$

$$G(s) = g_2 s^2 + g_1 s + g_0 \tag{29}$$

Additionally, $A(s)$ should be a fourth-order polynomial, which is:

$$A(s) = a_4 s^4 + a_3 s^3 + a_2 s^2 + a_1 s + a_0 \tag{30}$$

Then, there will be four unknowns in five equations, which will not give a minimal degree of solution. In order to solve this set of equations, an extra unknown τ can be introduced by setting the $A(s)$ as:

$$A(s) = (\varpi + 1)(a_{m3} s^3 + a_{m2} s^2 + a_{m1} s + a_{m0}) \tag{31}$$

Combining (17), (19), (20), (28), (29) and (31) gives:

$$\begin{bmatrix} 0 \\ a_{m3} \\ a_{m2} \\ a_{m1} \\ a_{m0} \end{bmatrix} = \begin{bmatrix} d_4 & n_2 & 0 & 0 & -a_{m3} \\ 0 & 0 & n_2 & 0 & -a_{m2} \\ d_2 & n_0 & 0 & n_2 & -a_{m1} \\ 0 & 0 & n_0 & 0 & -a_{m0} \\ d_0 & 0 & 0 & n_0 & 0 \end{bmatrix} \times \begin{bmatrix} f_0 \\ g_2 \\ g_1 \\ g_0 \\ \tau \end{bmatrix} \tag{32}$$

As in the last section, this can be solved for the *F(s)* and *G(s)* coefficients and the extra unknown τ. However, τ needs to be evaluated to ensure that it is always a positive value, which

means it is a stable poleposition. τ can be calculated from (32), which for the plant parameters in Table 1, gives:

$$\tau = -\frac{a_{m1}}{a_{m0} + 0.0095a_{m2}} - \frac{a_{m3}}{105.1349a_{m0} + a_{m2}} \quad (33)$$

Since t $A(s)$ is specified to represent stable poles, as a result, a_{m0}, a_{m1}, a_{m2} and a_{m3} are positive values. According to (33), τ is always negative. In another words, a pole in $A(s)$ is always placed in the right half plane, so the closed-loop system is not stable. Therefore, the jerk feedback cannot be cancelled or avoided in the controller.

5.2 Noise tolerance

The appearance of noise in physical circumstance would bring significant effect on the control performance of the system. As Fig. 9 shows, by implementing $H(s)$ as a forward compensator, (36) indicates that the reciprocal of $H(s)$ can be used as a filter to attenuate the noise.

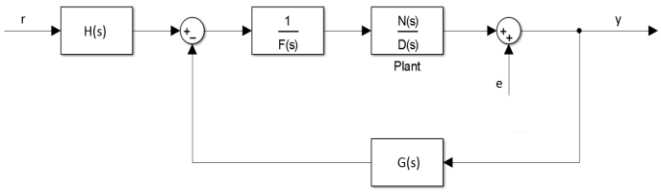

Fig. 9. Closed-loop block diagram with $H(s)$ filter

$$y = \frac{N(s)H(s)}{D(s)F(s) + N(s)G(s)}r + \frac{D(s)F(s)}{D(s)F(s) + N(s)G(s)}e \quad (34)$$

If,

$$D(s)F(s) + N(s)G(s) = A_m(s)H(s) \quad (35)$$

Substituting (35) into (34):

$$y = \frac{N(s)}{A_m(s)}r + \frac{D(s)F(s)}{A_m(s)H(s)}e \quad (36)$$

According to the previous discussion, $A_m(s)H(s)$ can be given by the polynomial with desired stable poles, and the steady state gain is calculated to give unity gain in the closed loop. If $H(s)$ is specified as the denominator of a second order low pass filter, which includes two roots of $A(s)$, it can be used to attenuate the noise without influencing the servo performance of the system. In order to give a unity steady state gain:

$$N(0) = A_m(0) \quad (37)$$

However, it is necessary to evaluate that if the noise will be amplified by using different $H(s)$. Fig. 10 is the noise amplitude against frequency according to different $H(s)$.

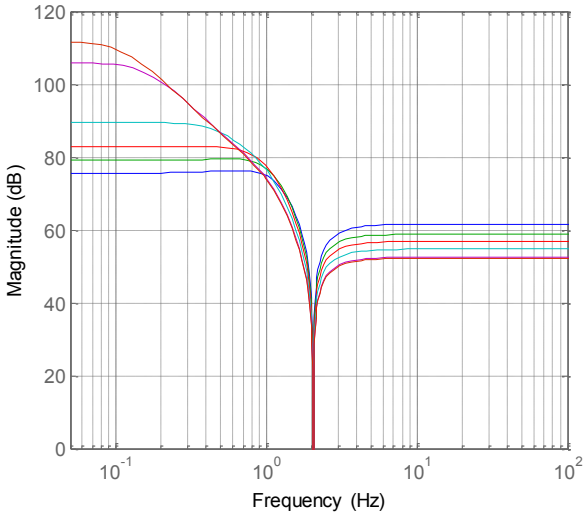

Fig. 10. Frequency response of output angel (y) to noise (e) for different cut-off frequency of $H(s)$, as 0.7 rad/s, 1 rad/s, 3 rad/s, 5 rad/s, 7 rad/s and 10 rad/s, respectively.

At high frequencies, there is no significant amplification of the noise, especially when $H(s)$ has faster response poles. However, another aspect need to be investigated is the frequency response of the control signal and noise, as Fig. 11 shows

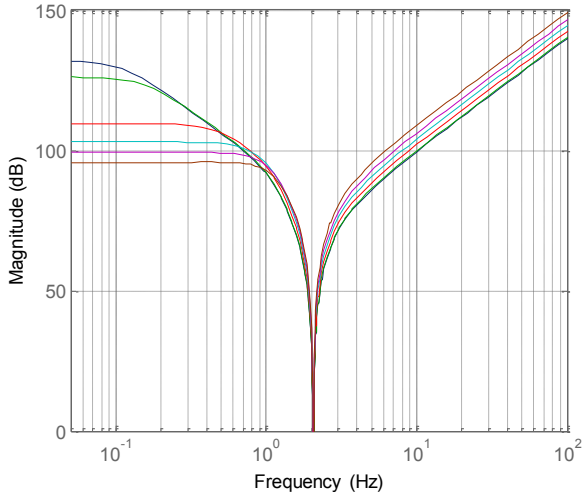

Fig. 11. Frequency response of control signal (u) to noise (e) for different cut-off frequency of $H(s)$, as 0.7 rad/s, 1 rad/s, 3 rad/s, 5 rad/s, 7 rad/s and 10 rad/s, respectively.

At high frequencies, the noise amplification is increasing dramatically. This leads to the discussion of the poles selection, which is a balance according to the investigation of the system`s performance (Chen, 1995).

6. CONCLUSIONS

The foot contact area is a significant criteria when considering the quiet standing position of a humanoid robot. Most of the successful bipedal robot maintain balance by improving the mechanical structure with the combination of ZMP control method. Investigation of the control of a small size bipedal

robot with point foot contact has been done in this paper. According to this specific configuration, pole-placement method is used to develop the controller. According to the calculation, the minimal degree of solution indicates the minimal number of feedback variables. Frequency response shows that the noise signal is not significantly amplified through all frequency band. However, the noise signal has a dramatically effect on the control signal.

An estimator or observer can be built to estimate state variables value without doing high demand of derivative calculations. According to hardware limitations, experimental results will be presented to demonstrate the feasibility of this controller in further research.

REFERENCES

Bottaro, A., Casadio, M., Morasso, P. G., & Sanguineti, V. (2005). Body sway during quiet standing: is it the residual chattering of an intermittent stabilization process?. *Human movement science*, 24(4), 588-615.

Chen, C. T. (1995). Linear system theory and design. *Oxford University Press*, Inc..

Erbatur, K., Okazaki, A., Obiya, K., Takahashi, T., & Kawamura, A. (2002). A study on the zero moment point measurement for biped walking robots. In Advanced Motion Control, 2002. *7th International Workshop on* (pp. 431-436). IEEE.

Hardarson, F. (1970). Locomotion for difficult terrain. *Dept. mach. des.*

Kajita, S. (1989). Method and apparatus for dynamic walking control of robot. *US, US4834200*.

Plummer, A. R. (1991). Digital control techniques for electro-hydraulic servosystems (Doctoral dissertation, University of Bath).

Raibert, M. (2010, December). Dynamic legged robots for rough terrain. In Humanoid Robots (Humanoids), *2010 10th IEEE-RAS International Conference on* (pp. 1-1). IEEE.

Sakagami, Y., Watanabe, R., Aoyama, C., Matsunaga, S., Higaki, N., & Fujimura, K. (2002). The intelligent ASIMO: System overview and integration. In Intelligent Robots and Systems, 2002. *IEEE/RSJ International Conference on* (Vol. 3, pp. 2478-2483). IEEE.